Nature Environment and Pollution Technology
An International Quarterly Scientific Journal

p-ISSN: 0972-6268
(Print copies up to 2016)
e-ISSN: 2395-3454

Vol. 24 | No. S1 | pp. 97-108 | 2025

Original Research Paper

https://doi.org/10.46488/NEPT.2025.v24iS1.006

Open Access Journal

Evaluation of the Photodegradation of Atrazine in the Presence of β-cyclodextrin Polymer: Experimental Design and Kinetic Study

O. S. Ayanda[1†], S. O. Adewuyi[1], S. M. Yahaya[2], O. Adeyi[3], S. M. Nelana[4] and M. J. Klink[4]

[1]Nanoscience Research Unit, Department of Industrial Chemistry, Federal University Oye Ekiti, P.M.B 373, Oye Ekiti, Ekiti State, Nigeria

[2]Department of Soil Science, Faculty of Agriculture/Institute for Agricultural Research, Ahmadu Bello University, P.M.B. 1044, Zaria, Nigeria

[3]Department of Chemical Engineering, Michael Okpara University of Agriculture, P.M.B 7267, Umudike, Abia State, Nigeria

[4]Department of Chemistry, Vaal University of Technology, South Africa

†Corresponding author: O. S. Ayanda; osayanda@gmail.com

Nat. Env. & Poll. Tech.
Website: www.neptjournal.com

Received: 05-05-2024
Revised: 06-06-2024
Accepted: 18-06-2024

Key Words:
Atrazine
β-cyclodextrin polymer
Photocatalysis
Ultraviolet irradiation
Thermogravimetric analysis

ABSTRACT

The degradation of atrazine (ATZ) was studied in the presence of β-cyclodextrin (β-CD) under ultraviolet light irradiation. The β-CD was characterized by modern analytical techniques and the different operating parameters of photodegradation were investigated. Experimental results revealed irregular shapes in the structure of β-CD, and the functional groups of β-CD were present in the glucose units. The BET surface area of β-CD was 285.02 m^2/g with a pore volume of 0.172 cc/g and a pore diameter of 2.138 nm, whereas, the x-ray diffraction analysis revealed the polycrystalline nature of β-CD. The z-average diameter of the particle size distribution was determined as 63.21 nm, thermogravimetric analysis data demonstrated weight loss events while the differential thermal analysis data revealed associated energy changes during phase transitions. The photodegradation of ATZ in the presence of β-CD resulted in 80.80% and 59.40% degradation, respectively, for 6.25 mg/L and 100 mg/L of ATZ after 60 min of irradiation time. The treatment method could be described by the Langmuir-Hinshelwood kinetic model, with k_c equals 0.1462 $mgL^{-1}min^{-1}$ and K_{LH} equals 10.45 × 10^{-2} Lmg^{-1}. Thus, photodegradation with β-CD as a catalyst could be effectively used for the remediation of pesticide-contaminated wastewater.

INTRODUCTION

β-cyclodextrin (β-CD) is an amphiphilic molecule with a hydrophobic inner cavity rich in electrons (Kasprzak & Poplawska 2018). It serves as a host molecule for the supramolecular inclusion of a variety of guest molecules which results in host-guest inclusion complexes (Duan et al. 2020, Morin-Crini et al. 2018). Thus, the application of β-CD for the selective eradication of organic pollutants is a possibility. The capability of β-CD has been noticed to promote the degradation of organic pollutants. In recent years, numerous studies have investigated the application of -CD in photocatalysis, revealing its prospect as an effective and versatile material for environmental remediation. One significant study was conducted by Liu et al. (2020), this comprehensive review highlights cyclodextrin-based adsorbents as assuring materials for wastewater treatment due to their outstanding physicochemical properties. This material shows excellent performance in removing heavy metals, dyes, endocrine-disrupting chemicals, and mixed pollutants from water. The photocatalytic decoloration of organic dyes (Velusamy et al. 2014), and organophosphorus pesticides (Kamiya et al. 2001) by β-CD has been reported. Liu et al. (2011) also reported the photocatalytic degradation of pesticides with sulfonated β-CD and in a work by Zhou et al. (2019), the adsorptive removal of carbamazepine, chloroxylenol, and bisphenol A from water through β-CD polymer has been investigated. Another significant contribution comes from the work of Zhang et al. (2021), the authors explored polyacrylonitrile/β-cyclodextrin composite nanofibrous membranes with TiO_2 and graphene oxide (GO) which were prepared via electrospinning. The results showed the highest photocatalytic efficiency under sunlight, degrading methyl blue (MB) (93.52 ± 1.83%) and methyl orange (MO) (90.92 ± 1.52%). This eco-friendly and reusable PAN/β-cyclodextrin/TiO_2/GO nanofibrous membrane holds

significant potential for the effective removal of dyes from industrial wastewaters.

A recent study by Yadav et al. (2022) delved into the various cyclodextrin-based materials such as composites, nanocomposites, polymers, hydrogels, membranes, and immobilized supports for diverse environmental applications. Cyclodextrin's eco-friendly nature promotes green processes, and the reversible equilibrium of the inclusion phenomenon allows for innovative pollutant removal techniques, including supramolecular chemistry, biodegradation, and advanced oxidation, enabling complete pollutant removal and cyclodextrin recycling. In a recent experimental study conducted by Jia et al. (2024), a novel nano-adsorbent, CD/CA-g-CS, was synthesized by chemically binding β-CD with chitosan (CS) and citric acid (CA) for efficient dye removal from wastewater. The material exhibited outstanding adsorption capacities for cationic and anionic dyes, surpassing previous adsorbents. CD/CA-g-CS demonstrated effective removal of mixed dyes in simulated sewage and real industrial wastewater, with an additional antibacterial activity of over 99.99% against E. coli, making it a promising solution for high-efficiency dyeing wastewater remediation. Conclusively, the collective results from these studies show the rising importance of β-CD in enhancing photocatalysis for environmental applications. The studies mentioned above provide important visions into the mechanisms over which β-CD improves photocatalytic efficiency and provide a foundation for further research in modifying β-CD based materials for particular environmental remediation challenges. As scientists continue to investigate the potential of β-CD in photocatalysis, these studies pave the technique for the development of novel and effective strategies for tackling environmental pollutants.

The herbicide atrazine (ATZ) is often used to manage weeds and has been found in surface and groundwater in many places throughout the world. ATZ is an endocrine disruptor that is frequently present in soil ecosystems where it accumulates because of its low volatility, delayed hydrolysis, high chemical stability, and poor biodegradability (Altendji & Hamoudi 2023). Therefore, addressing the deterioration of ATZ in water through appropriate methods is crucial. Therefore, the study aims to investigate the photocatalysis of ATZ using β-CD polymer as a photocatalyst. The objectives are (i) the characterization of β-CD polymer (ii) the investigation of the effect of operating conditions on the reaction advancement and (iii) the investigation of the kinetics and mechanism of photodegradation of ATZ by β-CD polymer. An innovative way to combat water pollution is by photocatalytic reaction, in which the catalyst and light source photon work in concert to break down the target pollutant.

MATERIALS AND METHODS

Chemical Reagents

β-CD polymer produced by Wacker CH was obtained from Sigma Aldrich. ATZ standard, (2-Chloro-4-ethylamino-6-isopropylamino-1,3,5-triazine) was also obtained from Sigma Aldrich. Other chemical and reagents include ethanol, sodium hydroxide and hydrochloric acid. Distilled water was used for all analytical preparations.

Instrumentations

Fourier transform infrared spectroscopy (FTIR) was used to determine the functional group present in β-CD polymer. The scanning electron microscope - energy dispersive X-ray spectroscopy (SEM-EDS) Phenon Prox model, manufactured by Phenom-World Eindhoven, Netherlands was used to carry out the morphology analysis. Other characterizations include x-ray diffraction (XRD) (Empyrean Malvern Panalytical Diffractometer), thermogravimetric analysis - differential thermal analysis (TGA-DTA) (PerkinElmer TGA 4000), Brunauer, Emmett, and Teller (BET) and particle size analysis.

Photocatalysis of Atrazine

The aqueous ATZ was photodegraded at ambient temperature in a photocatalytic reactor operating under ultraviolet (UV) light at a wavelength of 254 nm (Altendji & Hamoudi 2023). A mixture of 25 mL of ATZ solution and catalyst was vigorously stirred under UV light irradiation for 5 - 60 min in the dark. The aliquots were sampled and filtered to remove the solid phase. Detection of the concentration of ATZ was done by Shimadzu UV-1650 PC at a maximum wavelength of 220 nm (Assaker & Rima 2012). The degradation efficiency (%) was obtained using Equation 1 (Aremu et al. 2022).

$$\%Degradation = \frac{ATZ_0 - ATZ_t}{ATZ_0} \times 100 \quad ...(1)$$

where ATZ_0 and ATZ_t are the initial and final concentrations of ATZ, respectively.

RESULTS AND DISCUSSION

EDS and SEM Analysis of β-Cyclodextrin

The SEM image presented in Fig. 1a showcases the morphology of β-CD polymer. Notably, the image reveals irregular shapes in the structure of β-CD. This suggests that the β-CD polymer is not uniform in its structure. This variability can impact its properties and performance and it is indicative of the agglomeration or aggregation of β-CD particles. This observation aligns

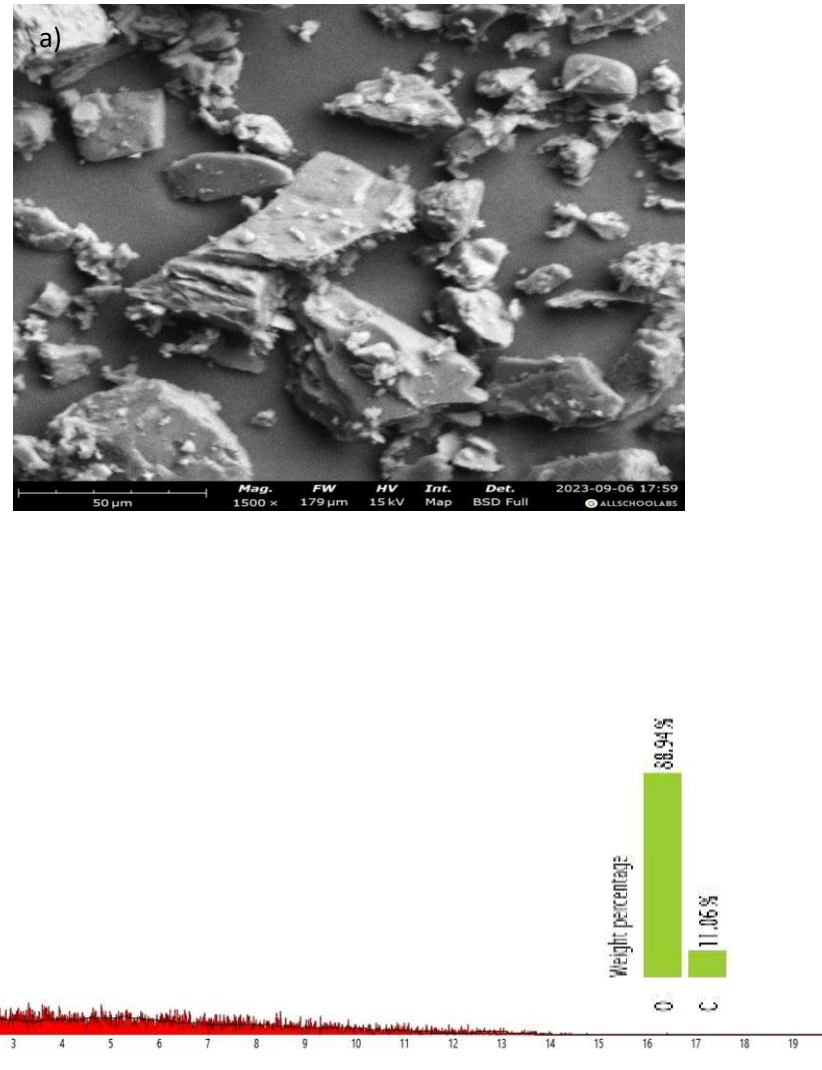

Fig. 1: SEM micrograph and EDS spectrum of β-cyclodextrin.

closely with the research findings reported by Rachmawati et al. (2013), which focused on the synthesis of molecular inclusion complexes involving curcumin and β-CD nanoparticles.

Fig. 1b illustrates the EDS spectrum obtained from the analysis of β-CD polymer. Within the figure, the spectrum qualitatively reveals the relative abundance of elements found in the β-CD sample. From this spectral data, two distinct elements emerge as being present in the β-CD, namely oxygen (O) and carbon (C). Notably, Fig. 1b underscores that oxygen (O) is the predominant element within the analyzed β-CD polymer. The analysis demonstrates that oxygen constitutes the majority of the composition at 88.94%, with carbon accounting for the remaining 11.06%.

TGA-DTA of β-Cyclodextrin Polymer

The TGA-DTA curves obtained for β-CD polymer provide valuable insights into the material's thermal behavior, with the DTA data offering a complementary perspective on the energy changes during phase transitions. Fig. 2 displays the TGA-DTA curve for β-CD polymer. Notably, a weight loss event is observed between 90.14°C and 90.32°C, resulting in a substantial reduction in weight from 99.997% to 96.356%. The TGA curve indicates a significant weight loss, typically associated with thermal decomposition or degradation. In the context of β-CD, this suggests that the sample undergoes decomposition, leading to the release of volatile components and a corresponding weight loss. The DTA data offer further insights into these observations. At around 32°C in the DTA curve, an endothermic peak is evident, indicating the

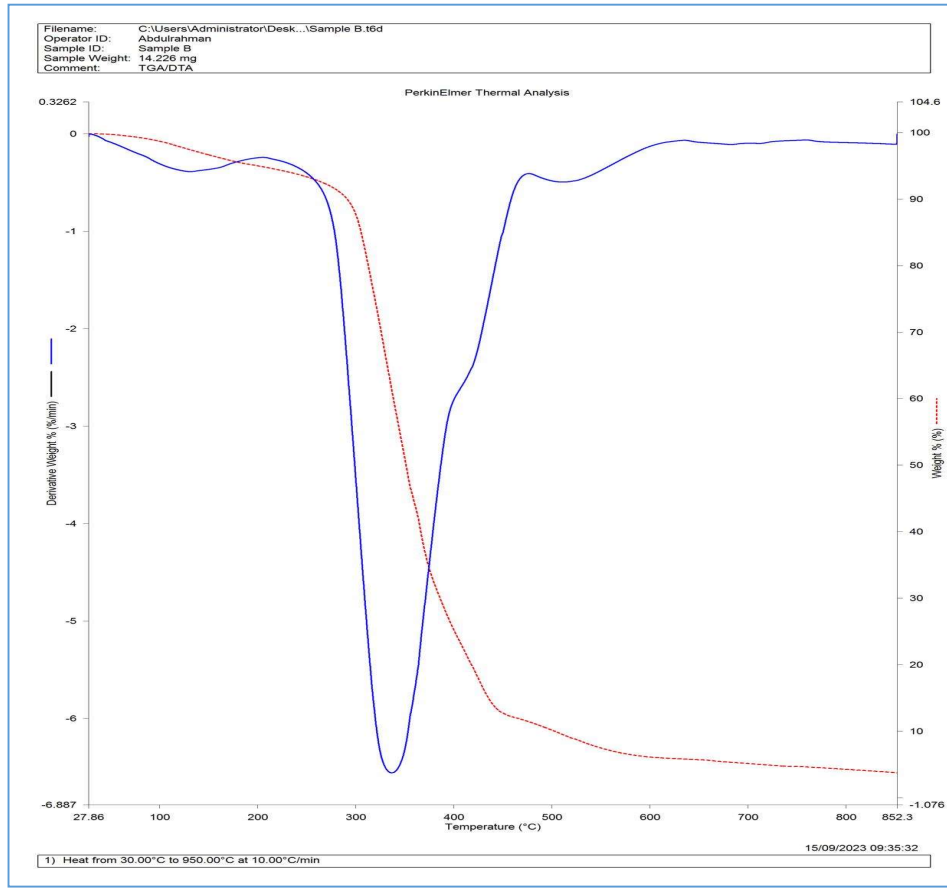

Fig. 2: TGA-DTA curves for β-cyclodextrin polymer.

absorption of heat during this phase transition such as melting or dehydration (Rajamohan et al. 2022). The endothermic nature of this peak confirms that energy is absorbed during the transition, consistent with the decomposition process indicated by the TGA data.

Subsequently, at approximately 38°C in the DTA curve, an exothermic peak is observed, signifying the release of heat. This corresponds to an exothermic phase transition, which in the context of β-CD, could be linked to crystallization or another exothermic process. The release of heat during this transition aligns with the weight loss and decomposition noted in the TGA data, further supporting the idea that significant changes are occurring within the materials. As we move to higher temperatures, the TGA data indicate two more weight loss events, one between approximately 290°C and 240°C and another between 417°C and 435°C. These events likely signify pronounced changes or decomposition in the β-CD sample. The DTA data continue to corroborate the TGA findings. Notably, an endothermic peak at 505°C is observed, indicating another energy-absorbing phase transition or process at this elevated temperature. This endothermic peak aligns with the weight loss events observed in the TGA data and further supports the idea of structural or phase transformations in the β-CD samples under extreme thermal conditions.

Fourier Transform Infra-Red Spectroscopy of β-Cyclodextrin

The FTIR spectrum of β-CD polymer (Fig. 3) shows peaks that correspond to the functional groups present in the glucose units of β-CD, such as C-H, C-O, and O-H bonds. These peaks are important for identifying β-CD. Fifteen (15) absorption bands were observed in the FTIR spectrum of β-CD and included bands observed at wavenumbers of 704.46 cm^{-1}, 752.92 cm^{-1}, 857.28 cm^{-1}, 939.28 cm^{-1}, 1021.29 cm^{-1}, 1077.20 cm^{-1}, 1151.74 cm^{-1}, 1252.38 cm^{-1}, 1334.38 cm^{-1}, 1367.93 cm^{-1}, 1416.38 cm^{-1}, 1640.02 cm^{-1}, 2102.21 cm^{-1}, 2929.68 cm^{-1} and 3265.14 cm^{-1}. The peaks obtained from the FTIR data of β-CD polymer are consistent with those reported in

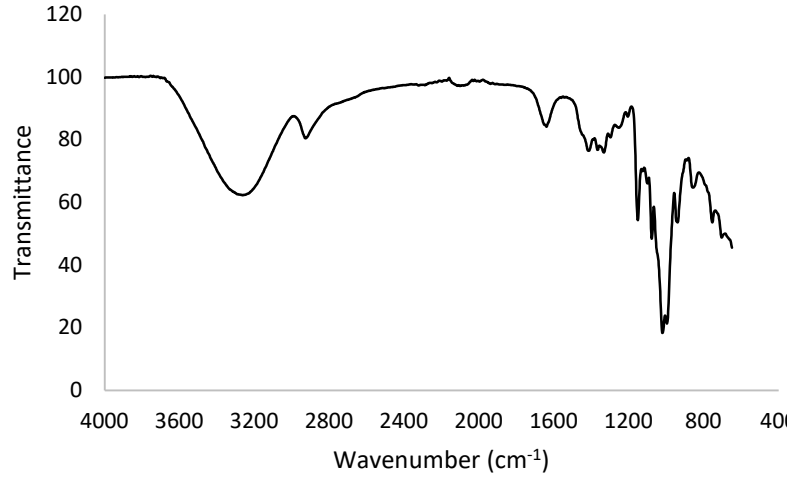

Fig. 3: FTIR spectrum of β-cyclodextrin.

the literature (Bratu et al. 2004, Sambasevam et al. 2013).

The FTIR data of the β-CD polymer were analyzed to assign the appropriate functional group to the various peaks. The peak at 704.46 cm^{-1} was attributed to the out-of-plane bending of C-H bonds in the glucose units of β-CD, while the peak at 752.92 cm^{-1} was assigned to the rocking vibration of C-H bonds in the glucose units of β-CD. The peaks at 857.28 cm^{-1}, 939.28 cm^{-1}, 1021.29 $cm^{-1,}$ 1077.20 cm^{-1}, 1151.74 cm^{-1}, and 1252.38 cm^{-1} were attributed to the stretching vibration of C-O bonds in the glucose units of β-CD. The peaks at 1334.38 cm^{-1}, 1367.93 cm^{-1}, and 1416.38 cm^{-1} were assigned to the stretching and bending vibrations of C-H bonds in the glucose units of β-CD. The peak at 1640.02 cm^{-1} was assigned to the stretching vibration of O-H bonds in the glucose units of β-CD. The peak at 2102.21 cm^{-1} was attributed to the stretching vibration of C≡C bonds typically found in alkynes. The peaks at 2929.68 cm^{-1} and 3265.14 cm^{-1} were assigned to the stretching vibration of C-H and O-H bonds in the glucose units of β-CD, respectively (Rachmawati et al. 2013). The identification of functional groups in the FTIR data of β-CD polymer is important for understanding its molecular structure and properties.

BET Analysis and Particle Size Distribution of β-Cyclodextrin

Fig. 4 shows the BJH cumulative pore distribution of β-CD. β-CD exhibited a surface area of 285.02 m^2/g. The pore size was determined by the Barrette-Joyner-Halenda (BJH) method. The pore volume of β-cyclodextrin was 0.172 cc/g, it exhibits a slightly larger pore diameter of 2.138 nm.

Fig. 5 illustrates the particle size distribution of β-CD, revealing a broad spectrum of particle sizes ranging from as small as 0.4 nm to as large as 10,000 nm (or 10 μm). This distribution is characterized by two key parameters: particle size, expressed in nanometers, representing the physical dimensions of β-CD particles, and intensity, denoted in percentage, which signifies the relative abundance of particles within specific size intervals. As depicted in the figure, there is a noticeable trend in the intensity values as particle size increases, signifying variations in the relative abundance of particles across different size ranges. The z-average diameter of this distribution is determined to be 63.21 nm, indicating that the mean size of β-CD particles within the sample falls within this size range. The obtained value of 63.21 nm is far lower than the 173.212 μm reported for hydroxypropyl-β-cyclodextrin (Li et al. 2018). Crucially, the distribution curve unveils the presence of three distinct peaks, a characteristic feature of a multimodal distribution. These peaks represent separate populations of β-CD particles, each characterized by unique sizes and relative abundances.

The first and most prominent peak, centered at approximately 102.8 nm, exhibits a high intensity of 83.5%, signifying a substantial concentration of β-CD particles within this size range. Notably, this peak displays a relatively wide standard deviation of 130.5 nm, indicating notable variability in the sizes of β-CD particles within this particular range. Conversely, the second peak, located around 2.319 nm, displays a lower intensity of 8.5%. This peak represents a population of considerably smaller β-CD particles. Remarkably, the standard deviation for this peak is remarkably low at 1.606 nm, suggesting a high degree of uniformity in particle size, with particles tightly clustered

around the mean. Lastly, the third peak, characterized by a z-average diameter of 3528 nm and an intensity of 5.1%, corresponds to larger β-CD particles. Analogous to the first peak, this segment also exhibits a relatively large standard deviation of 1280 nm, indicating considerable variation and heterogeneity in particle sizes within this range. In summary, the particle size distribution data of β-CD underscores the diverse nature of particle sizes within the sample. The presence of multiple peaks signifies the coexistence of distinct populations of β-CD particles with varying sizes and relative abundances. This data is pivotal for tailoring β-CD for specific applications where particle size plays a crucial role, such as drug delivery systems, encapsulation, and other innovative uses in pharmaceuticals and materials science.

XRD Pattern of β-Cyclodextrin

XRD analysis was harnessed to delve into the intricate realm of phase composition and crystallite structure within the

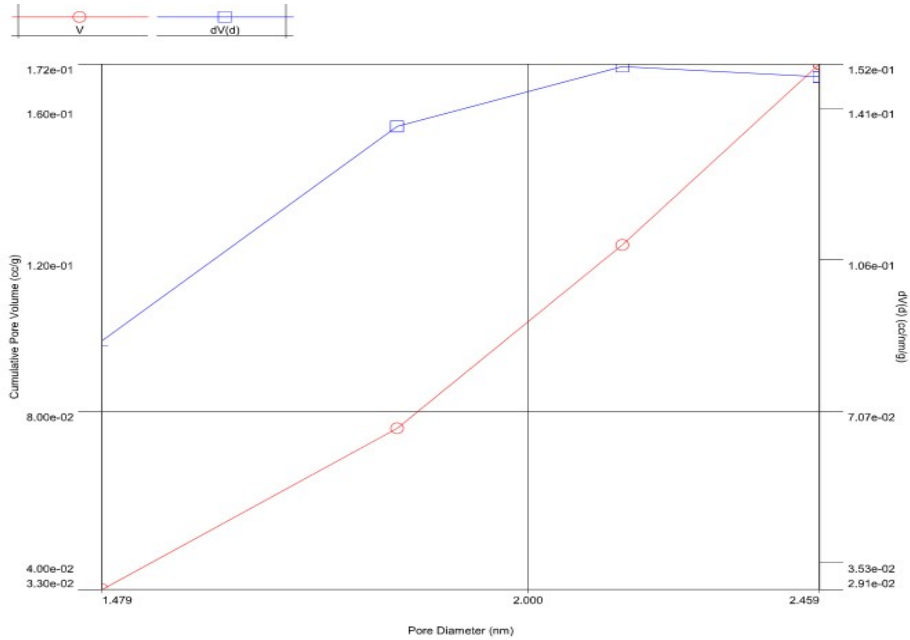

Fig. 4: BJH pore size distribution of β-cyclodextrin.

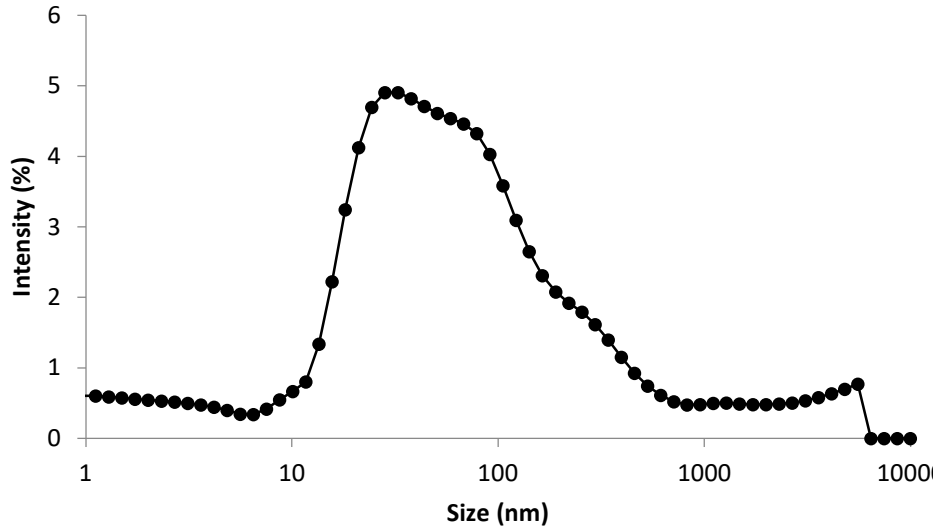

Fig. 5: Particle size distribution of β-cyclodextrin.

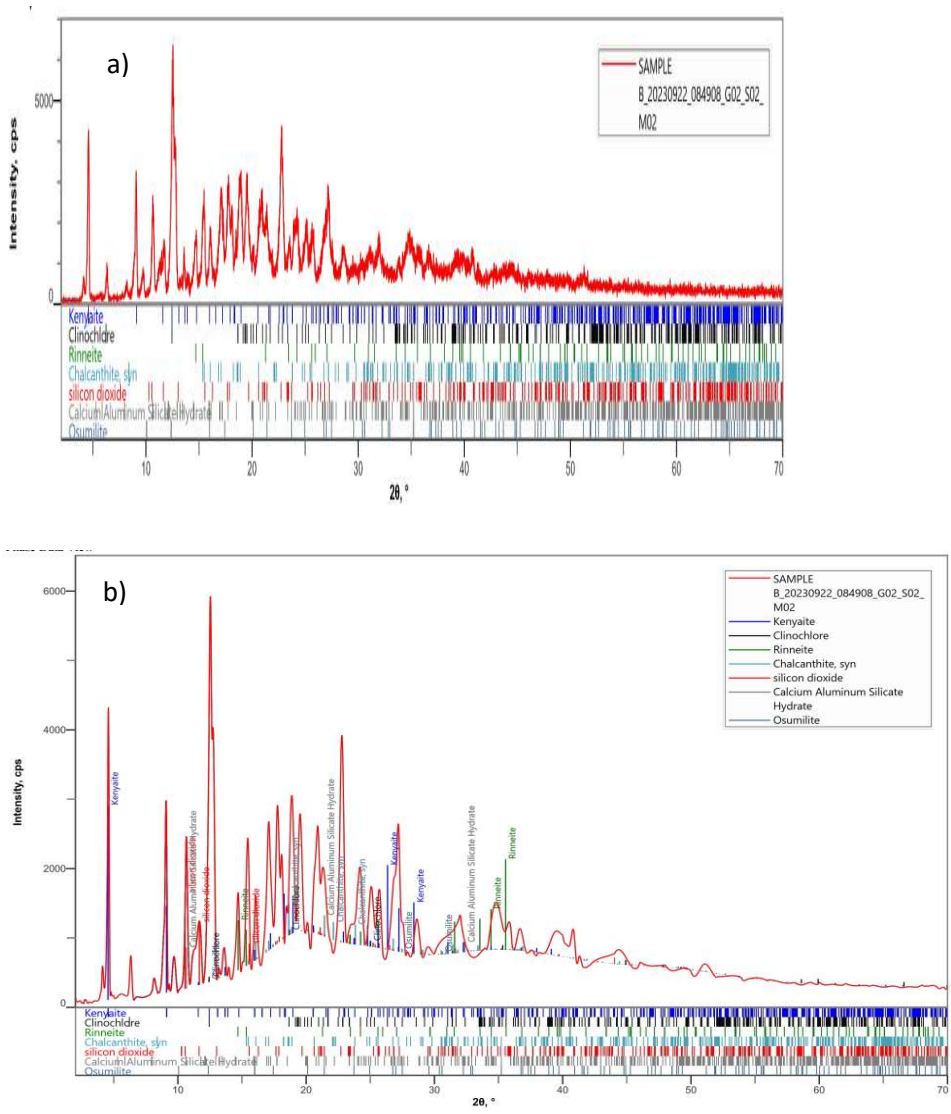

Fig. 6: XRD pattern of β-cyclodextrin (a), and β-cyclodextrin matched with standard (JCPDS card file).

XRD pattern of β-CD polymer. The findings, prominently featured in Fig. 6a unveiled a vivid portrayal of the XRD pattern of β-CD, covering a 2θ range from 0° to 70°. This XRD analysis astutely revealed the polycrystalline nature of β-CD, as evidenced by the presence of multiple peaks at various 2θ angles. This observation aligns harmoniously with previous research, as supported by the work of Musuc et al. (2020). In the XRD patterns of β-CD, a total of thirty-three (33) distinguishable peaks graced the spectrum. However, seven of these peaks stood out as particularly prominent. Positioned at 2θ angles of 4.600°, 9.0620°, 12.53°, 12.767°, 17.78°, 22.783°, and 27.08°, these peaks were accompanied by integrated intensities of 50, 447, 626, 923, 511, 675, and 597 counts per second (cps) respectively. Notably, the 2θ values corresponding to these peaks closely mirrored the findings presented by Musuc et al. (2020).

Fig. 6b presents a comprehensive XRD analysis of β-CD polymer, thoughtfully compared with established standards, specifically the JCPDS card 00-054-1476. This analytical approach sought to unravel the phase composition and crystallite structure of the material, providing critical insights into its underlying characteristics. The findings depicted in Fig. 6b offer a compelling depiction of the XRD pattern of β-CD, extending over a 2θ range. What becomes apparent from this examination is the striking resemblance between the analyzed sample's XRD pattern and the reference standard for β-CD decahydrate ($C_{42}H_{70}O_{35}$-$C_7H_7NO_2$•$10H_2O$) as

represented by the JCPDS card 00-054-1476. The XRD analysis indicates that all the diffraction peaks present in the sample's pattern are consistent with the monoclinic structure of β-CD decahydrate, further confirming its identity. This alignment between the sample's XRD pattern and the standard is significant, as it unequivocally establishes that the material under analysis is indeed β-CD decahydrate. The distinct peaks, their positions, and the overall pattern concur with the established reference, reinforcing the identity of the material.

Photocatalysis of Atrazine by β-Cyclodextrin

Effect of the irradiation time and β-cyclodextrin dosage: In the photocatalytic degradation of the ATZ using β-CD, the results demonstrate a dosage-dependent impact on the photocatalytic degradation over the specified time intervals (Fig. 7). The lowest dosage of 0.1g β-CD at 5 minutes exhibited the lowest degradation efficiency of 6.2%, while the highest dosage of 0.5 g exhibited a higher degradation of 17.6%. This trend continued through the subsequent time of the study, with the 0.5 g dosage consistently outperforming the 0.1 g dosages. Remarkably, at 60 minutes, the 0.1 g dosage caused 47.4% degradation, while the 0.5g dosage attained a moderately higher degradation efficiency of 59.4%.

Kinetics of Degradation

By assuming pseudo-first-order reaction kinetics, Equation 2 was used to deduce the photocatalytic rate constants (Ayanda et al. 2021).

$$-\frac{dATZ}{dt} = kATZ \Leftrightarrow \ln\left(\frac{ATZ_0}{ATZ_t}\right) = kt \qquad \ldots(2)$$

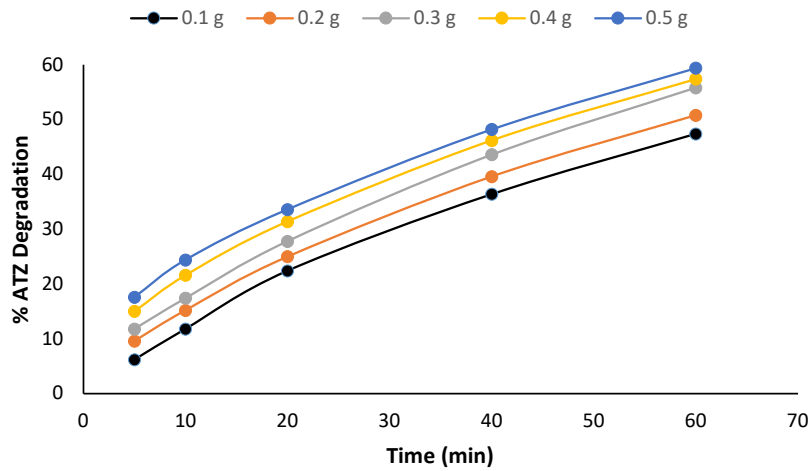

Fig. 7: Effect of the irradiation time and β-cyclodextrin dosage on the photocatalytic degradation of atrazine. *Experimental Condition:* Atrazine concentration = 50 mg/L, Volume of solution = 25 mL, Time = 5-60min, Nanomaterials dosage = 0.1-0.5g.

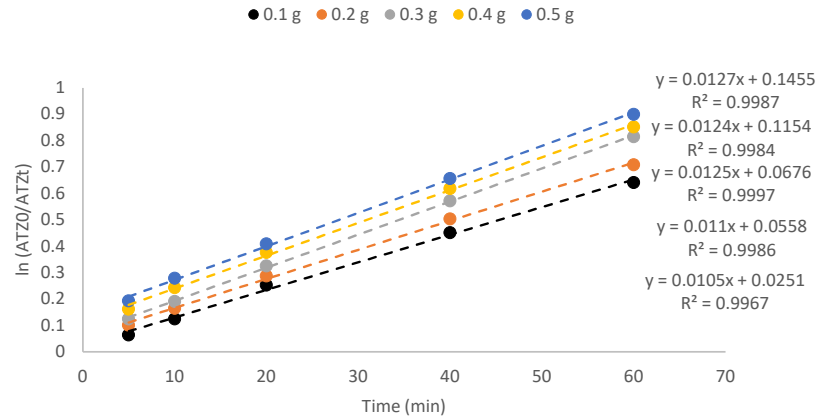

Fig. 8: Kinetics of atrazine photocatalytic degradation.

The kinetic plot is shown in Fig. 8. The removal of ATZ with variation in β-**CD** dosage (0.1-0.5 g) best fits pseudo-first-order kinetics with rate constants k and R^2 values of 0.0105 min^{-1}, 0.011 min^{-1}, 0.0125 min^{-1}, 0.0124 min^{-1} and 0.0127 min^{-1}. The R^2 values are 0.9967, 0.9986, 0.9997, 0.9984 and 0.9987, respectively.

Effect of Initial Concentration of Atrazine

For β-CD degradation of ATZ considering the initial concentration of ATZ, the results also reveal a concentration-dependent trend, showcasing that, higher initial concentrations of ATZ result in decreased degradation efficiencies (Fig. 9). For instance, at the lowest concentration of 6.25 mg/L, degradation rates were 28.0% at 5 minutes to 80.8% at 60 minutes. As the initial concentration increases to 100 mg/L, the resultant degradation rates decrease, ranging from 15.0% at 5 minutes to 59.4% at 60 minutes. This outcome aligns with common observations in photocatalysis, where higher initial concentrations can lead to increased competition for active sites on the catalyst surface, potentially affecting the overall efficiency of the photocatalytic process (Bagheri et al. 2017, Østergaard et al. 2024, Rehan et al. 2024).

Mechanism of degradation: The degradation of ATR by UV light catalyzed by β-CD followed the pseudo-first-order kinetics and depended on the concentration of ATR in the bulk solution (Equation 3). The integration of Equation 3 leads to Equation 4. Fig. 10 represents a plot of

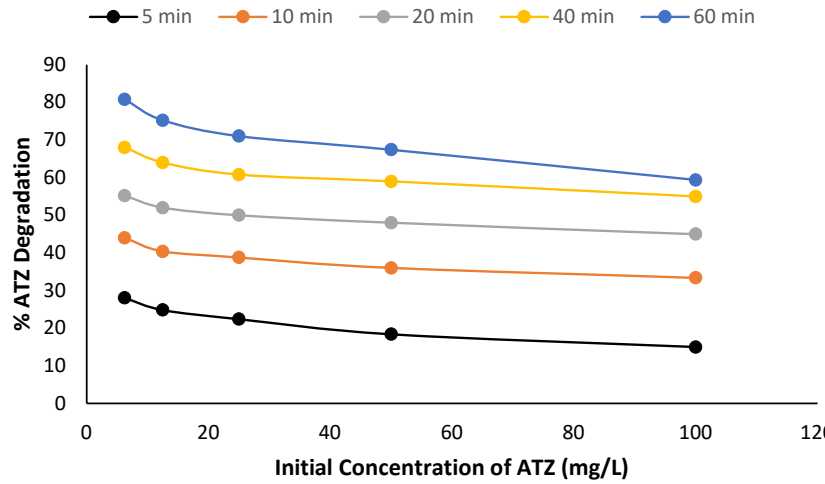

Fig. 9: Effect of initial concentration of atrazine. *Experimental Condition:* Atrazine concentration = 6.25-100 mg/L, Volume of solution = 25 mL, Time = 5-60min, Nanomaterials dosage = 0.5g.

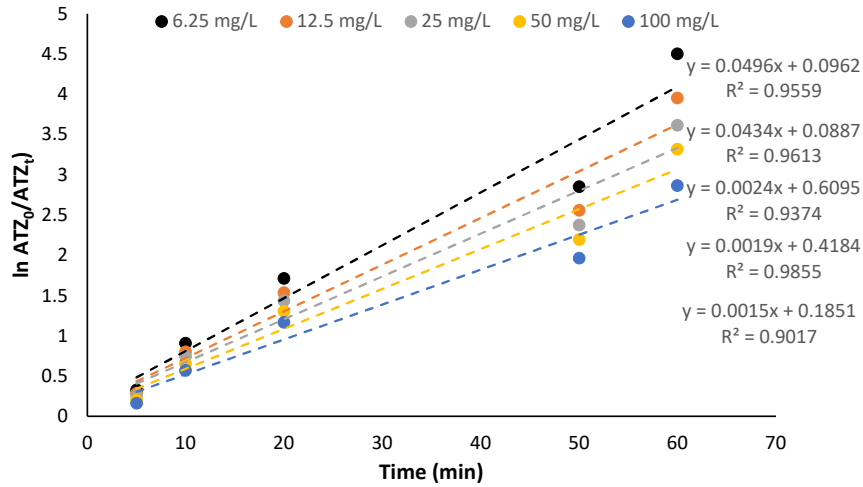

Fig. 10: Plot of $\ln\left(\frac{ATZ_o}{ATZ_t}\right)$ vs Time.

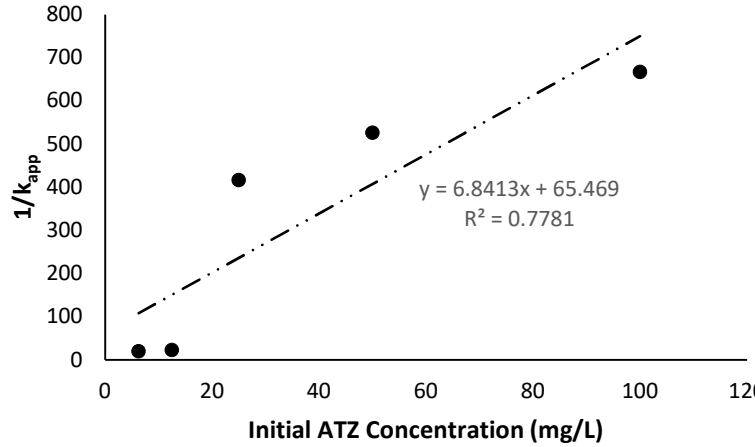

Fig. 11: Langmuir-Hinshelwood kinetic plot.

$\ln\left(ATZ_o/ATZ_t\right)$ vs t.

$$r = -\frac{dATZ}{dt} = k_{app}t \quad \ldots(3)$$

$$\ln\left(\frac{ATZ_o}{ATZ_t}\right) = k_{app}t \quad \ldots(4)$$

The apparent pseudo-first-order rate constants obtained from the Langmuir–Hinshelwood model for UV light-catalyzed degradation of ATZ using β-CD, signified by k_c 0.1462 $mgL^{-1}min^{-1}$ and K_{LH} 10.45×10^{-2} Lmg^{-1} (Table 1), gave important understandings into the mechanism of the reaction. The relatively higher K_{LH} and lower k_c values imply a substantial adsorption affinity and a moderate degradation rate, implying that the degradation efficiency is influenced by the adsorption of the reactant onto the β-CD surface (Jerjes et al. 2020). This result underlines the potential of β-CD as a catalyst in UV light-induced degradation reactions.

To determine the mechanism of action of the UV light catalyzed by β-CD, a heterogeneous kinetic model

Table 1: The apparent pseudo-first-order rate constants (*kapp*), R^2, and Langmuir–Hinshelwood model constants.

Atrazine (mg/L)	Rate Equations	K_{app} (min^{-1})	R^2	k_c (mg/L/min)	K_{LH} (L/mg)
6.25	0.0496x + 0.0962	0.0496	0.9559	0.1462	10.45×10^{-2}
12.5	0.0434x + 0.0887	0.0434	0.9613		
25	0.0024x + 0.6095	0.0024	0.934		
50	0.0019x + 0.4184	0.0019	0.9855		
100	0.0015x + 0.1851	0.0015	0.9017		

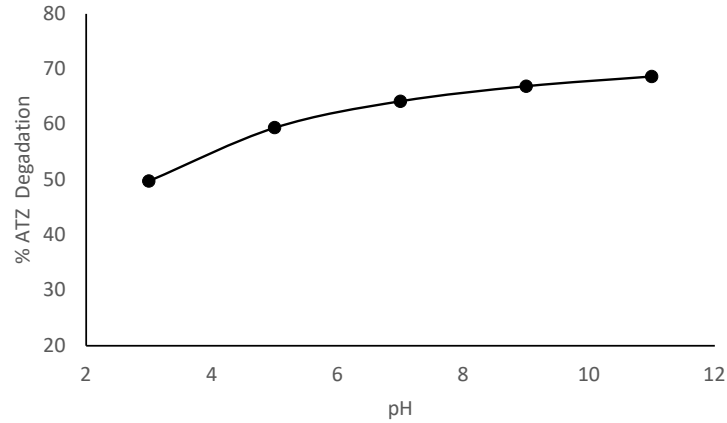

Fig. 12: Effect of pH on the photocatalytic degradation of atrazine. *Experimental Condition:* Atrazine concentration = 50 mg/L, Volume of solution = 25 mL, Time = 60min, Nanomaterials dosage = 0.5g.

(Equation 5) based on a Langmuir-Hinshelwood (L-H) model was applied (Ayanda et al. 2022), as presented in Fig. 11.

$$\frac{1}{k_{app}} = \frac{1}{k_c K_{LH}} + \frac{ATZ_o}{k_c} \quad \ldots(5)$$

The apparent pseudo-first-order rate constants (*kapp*), R^2 values, and the Langmuir-Hinshelwood model constants are presented in Table 1.

Effect of pH: Examining the influence of pH on the photocatalytic degradation of ATZ using β-CD also revealed an interesting result (Fig. 12). The results show that at pH 3, the lowest degradation of 49.76% was observed, signifying that the acidic conditions may have disturbed the photocatalytic activity of β-CD. As the pH increases, there is a steady increase in degradation efficiency, with pH 5 resulting in 59.4%, pH 7-64.2%, pH 9-66.9%, and the highest degradation observed at pH 11 with 68.7%.

This pH-dependent pattern supports the general understanding of photocatalytic reactions, where the surface charge of the catalyst and the nature of reactive species can be influenced by the pH of the solution (Li et al. 2019).

CONCLUSIONS

Cyclodextrins are cyclic oligosaccharides that have a high capacity for molecular inclusion. Within the discipline of environmental chemistry, cyclodextrins have been observed for their capacity to facilitate the breakdown of contaminants in aqueous solutions. Therefore, this study involved the detailed characterization of β-CD polymer, followed by the photocatalytic degradation of ATZ using β-CD polymer as a catalyst. The EDS analysis revealed oxygen (O) and carbon (C) as the main constituents of the β-CD. The identification of functional groups by FTIR helped to understand the molecular structure and properties of β-CD. The surface area of β-CD was 285.02 m^2/g with the z-average diameter determined as 63.21 nm. The XRD analysis indicated that all the diffraction peaks present in the sample's pattern are consistent with the monoclinic structure of β-CD decahydrate. The TGA data demonstrate weight loss events, suggesting decomposition or significant changes in β-CD, while the DTA data reveal associated energy changes during phase transitions. The endothermic and exothermic peaks in the DTA curve align with the weight loss events observed in the TGA data, providing a comprehensive and coherent understanding of β-CD's thermal behavior.

The remediation studies demonstrated a dosage-dependent impact on the photocatalytic degradation over the specified time intervals, and considering the initial concentration of ATZ, the results revealed a concentration-dependent trend, showcasing that, higher initial concentrations of ATZ result in decreased degradation efficiencies. The photodegradation of ATZ in the presence of β-CD is pH-dependent i.e., a higher percentage degradation was observed at higher pH when compared to a lower pH of ATZ solution. The highest degradation efficiency of 80.80% was achieved when 25mL of 6.25 mg/L of ATZ was subjected to UV irradiation in the presence of 0.5 g of β-CD for 60 min. This study has shown that ATZ can be effectively treated with UV light and β-CD polymer as a photocatalyst.

REFERENCES

Altendji, K. and Hamoudi, S., 2023. Efficient photocatalytic degradation of aqueous atrazine over graphene-promoted g-C_3N_4 nanosheets. *Catalysts*, 13(9), p.1265.

Aremu, O.H., Akintayo, C.O., Nelana, S.M., Klink, M.J. and Ayanda, O.S., 2022. Optimization of influential parameters for the degradation of metronidazole contained in aquaculture effluent via sonocatalytic process: kinetics and mechanism. *Nature Environment and Pollution Technology*, 21(4), pp.1875-1885.

Assaker, K. and Rima, J., 2012. Improvement of spectrophotometric method for the determination of atrazine in contaminated water by inducing of Mannich reaction. *Journal of Food Research*, 1(4), p.17.

Ayanda, O.S., Aremu, O.H., Akintayo, C.O., Sodeinde, K.O., Igboama, W.N., Oseghe, E.O. and Nelana, S.M., 2021. Sonocatalytic degradation of amoxicillin from aquaculture effluent by zinc oxide nanoparticles. *Environmental Nanotechnology, Monitoring & Management*, 16, p.100513.

Ayanda, O.S., Oforkansi, C.C., Aremu, O.H., Ogunjemiluyi, O.E., Olowoyeye, O.L. and Akintayo, C.O., 2022. Degradation of amido black dye using ultra-violet light catalyzed by iron oxide nanoparticles: kinetics and mechanism of degradation. *Catalysis Research*, 2(3), pp.1-11.

Bagheri, S., TermehYousefi, A. and Do, T.O., 2017. Photocatalytic pathway toward degradation of environmental pharmaceutical pollutants: structure, kinetics and mechanism approach. *Catalysis Science & Technology*, 7(20), pp.4548-4569.

Bratu, I., Veiga, F., Fernandes, C., Hernanz, A. and Gavira, J.M., 2004. Infrared spectroscopic study of triacetyl-β-cyclodextrin and its inclusion complex with nicardipine. *Spectroscopy*, 18(3), pp.459-467.

Duan, Z., Zhang, M., Bian, H., Wang, Y., Zhu, L., Xiang, Y. and Xia, D., 2020. Copper (II)-β-cyclodextrin and CuO functionalized graphene oxide composite for fast removal of thiophenic sulfides with high efficiency. *Carbohydrate Polymers*, 228, p.115385.

Jerjes, W., Theodossiou, T.A., Hirschberg, H., Høgset, A., Weyergang, A., Selbo, P.K., Hamdoon, Z., Hopper, C. and Berg, K., 2020. Photochemical internalization for intracellular drug delivery. From basic mechanisms to clinical research. *Journal of Clinical Medicine*, 9(2), p.528.

Jia, J., Wu, D., Yu, J., Gao, T., Guo, L. and Li, F., 2024. Upgraded β-cyclodextrin-based broad-spectrum adsorbents with enhanced antibacterial property for high-efficient dyeing wastewater remediation. *Journal of Hazardous Materials*, 461, p.132610.

Kamiya, M., Kameyama, K. and Ishiwata, S., 2001. Effects of cyclodextrins on photodegradation of organophosphorus pesticides in humic water. *Chemosphere*, 42(3), pp.251-255.

Kasprzak, A. and Poplawska, M., 2018. Recent developments in the synthesis and applications of graphene-family materials functionalized with cyclodextrins. *Chemical Communications*, 54(62), pp.8547-8562.

Li, C., Huang, Y., Dong, X., Sun, Z., Duan, X., Ren, B., Zheng,

S. and Dionysiou, D.D., 2019. Highly efficient activation of peroxymonosulfate by natural negatively-charged kaolinite with abundant hydroxyl groups for the degradation of atrazine. *Applied Catalysis B: Environmental*, 247, pp.10-23.

Li, Y., He, Z.D., Zheng, Q.E., Hu, C. and Lai, W.F., 2018. Hydroxypropyl-β-cyclodextrin for delivery of baicalin via inclusion complexation by supercritical fluid encapsulation. *Molecules*, 23(5), p.1169.

Liu, Q., Zhou, Y., Lu, J. and Zhou, Y., 2020. Novel cyclodextrin-based adsorbents for removing pollutants from wastewater: A critical review. *Chemosphere*, 241, p.125043.

Liu, Z.B., Yang, C. and Zhao, S.C., 2011. Research of photocatalytic degradation of pesticide with sulfonated β-cyclodextrin. *Advanced Materials Research*, 183, pp.1442-1445.

Morin-Crini, N., Fourmentin, M., Fourmentin, S., Torri, G. and Crini, G., 2018. Silica materials containing cyclodextrin for pollutant removal. *Cyclodextrin Applications in Medicine, Food, Environment and Liquid Crystals*, pp.149-182.

Musuc, A.M., Anuta, V., Atkinson, I., Popa, V.T., Sarbu, I., Mircioiu, C., Abdalrb, G.A., Mitu, M.A. and Ozon, E.A., 2020. Development and characterization of orally disintegrating tablets containing a captopril-cyclodextrin complex. *Pharmaceutics*, 12(8), p.744.

Østergaard, M.B., Egea-Corbacho, A., Wang, D., Deganello, F., Boffa, V. and Jørgensen, M.K., 2024. A self-cleaning thermocatalytic membrane for bisphenol A abatement and fouling removal. *Journal of Membrane Science*, 693, p.122336.

Rachmawati, H., Edityaningrum, C.A. and Mauludin, R., 2013. Molecular inclusion complex of curcumin–β-cyclodextrin nanoparticle to enhance curcumin skin permeability from hydrophilic matrix gel. *AAPS PharmSciTech*, 14, pp.1303-1312.

Rajamohan, R., Raorane, C.J., Kim, S.C. and Lee, Y.R., 2022. One pot synthesis of copper oxide nanoparticles for efficient antibacterial activity. *Materials*, 16(1), p.217.

Rehan, M., Montaser, A.S., El-Shahat, M. and Abdelhameed, R.M., 2024. Decoration of viscose fibers with silver nanoparticle-based titanium-organic framework for use in environmental applications. *Environmental Science and Pollution Research*, pp.1-22.

Sambasevam, K.P., Mohamad, S., Sarih, N.M. and Ismail, N.A., 2013. Synthesis and characterization of the inclusion complex of β-cyclodextrin and azomethine. *International Journal of Molecular Sciences*, 14(2), pp.3671-3682.

Velusamy, P., Pitchaimuthu, S., Rajalakshmi, S. and Kannan, N., 2014. Modification of the photocatalytic activity of TiO_2 by β-Cyclodextrin in decoloration of ethyl violet dye. *Journal of Advanced Research*, 5(1), pp.19-25.

Yadav, M., Thakore, S. and Jadeja, R., 2022. A review on remediation technologies using functionalized cyclodextrin. *Environmental Science and Pollution Research*, 29(1), pp.236-250.

Zhang, R., Ma, Y., Lan, W., Sameen, D.E., Ahmed, S., Dai, J., Qin, W., Li, S. and Liu, Y., 2021. Enhanced photocatalytic degradation of organic dyes by ultrasonic-assisted electrospray TiO_2/graphene oxide on polyacrylonitrile/β-cyclodextrin nanofibrous membranes. *Ultrasonics Sonochemistry*, 70, p.105343.

ORCID DETAILS OF THE AUTHORS

O. S. Ayanda: https://orcid.org/0000-0001-8022-8010
S. M. Yahaya: https://orcid.org/0000-0002-0159-8740
O. Adeyi: https://orcid.org/0000-0003-3479-5318
M. J. Klink: https://orcid.org/0000-0002-9131-6312